

Microlensing 2000: A New Era of Microlensing Astrophysics
ASP Conference Series, Vol. 000, 2000
J.W. Menzies and P.D. Sackett, eds.

Pixel lensing towards M31 in principle and in practice

Eamonn Kerins for the POINT-AGAPE Collaboration

*Theoretical Physics, University of Oxford,
1 Keble Road, Oxford OX1 3NP, UK*

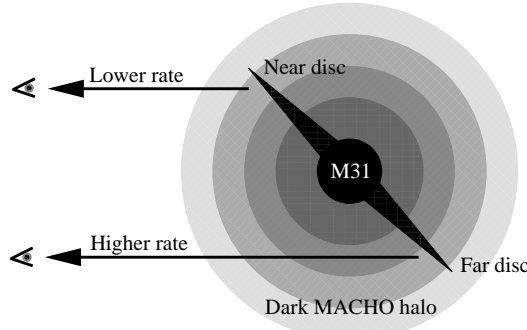
Abstract. The Andromeda galaxy (M31) provides a new line of sight for Galactic MACHO studies and also a signature, near-far asymmetry, which may establish the existence of MACHOs in the M31 halo. We outline the principles behind the so-called “pixel-lensing” experiments monitoring unresolved stars in M31. We present detailed simulations of the POINT-AGAPE survey now underway, which is using the INT wide-field camera to map the microlensing distribution over a substantial fraction of the M31 disc. We address the extent to which pixel-lensing observables, which differ from those of classical microlensing, can be used to determine the contribution and mass of M31 MACHOs. We also present some preliminary light-curves obtained from the first season (1999/2000) of INT data.

1. Andromeda: the new frontier

This meeting is in part a celebration of the success of the current pioneering generation of microlensing surveys, the discoveries of which are reported throughout these proceedings. However, as with all pioneering work, a number of puzzles remain to be solved including, crucially, whether MACHOs exist or whether current results towards the Large and Small Magellanic Clouds (LMC and SMC) can be explained by ordinary stellar populations. Whilst the MACHO Collaboration interprets the excess of events it finds as evidence of a $\sim 20\%$ halo contribution in objects of $\sim 0.5 M_{\odot}$ (Alcock et al. 2000) the EROS Collaboration has chosen to place only upper limits on the halo fraction from its sample of LMC/SMC events, even though the EROS dataset is formally consistent with that of MACHO (Lasserre et al. 2000). This dichotomy in approach reflects a community-wide uncertainty as to the contribution to the microlensing rate from the Magellanic Clouds themselves. As the current LMC/SMC surveys come to an end it is possible that the Magellanic satellite galaxies will continue to represent clouds of uncertainty for MACHOs.

Crotts (1992) and Baillon et al. (1993) proposed searching for MACHOs towards the Andromeda galaxy (M31). There are several aspects which make M31 very appealing for microlensing studies. Firstly, it is a large external galaxy, with $\mathcal{O}(10^{10})$ sources, and has a halo of its own, providing an additional site for MACHOs. We should therefore expect many more events than towards the Magellanic Clouds. Small number statistics ought not be an issue for M31 if the MACHO abundance is significant. Secondly, the additional line of sight through

Figure 1. The concept of near-far asymmetry. Due to the tilt of the M31 disc the microlensing rate is larger towards the far disc than towards the near side if MACHOs are present in a spheroidal dark halo. The effect is less pronounced if the halo is flattened. The distributions of disc events and variable stars are symmetric.



our own halo that M31 provides may help to decide the viability of some of the stellar self-lensing scenarios, which have been proposed as non-MACHO alternatives to explain the LMC/SMC events. Alcock et al. (1995) have also noted that the ratio of microlensing rates between M31 and the LMC could be used in principle to probe the outer rotation curve of our Galaxy, though in practice the background from events in M31 makes this difficult. Lastly, our external viewpoint is advantageous in that we can map the MACHO distribution across the face of the M31 disc. The importance of this has been emphasized by Crotts (1992), who noted that the 77° inclination of the M31 disc should give rise to a noticeable gradient in the microlensing rate if MACHOs occupy a spheroidal distribution, as depicted in Figure 1. Such an asymmetry does not arise naturally for disc lensing or variable stars, and so would provide strong evidence for the existence of MACHOs if detected.

2. Pixel lensing

There are a number of difficulties in conducting a ground-based programme towards more distant targets like Andromeda. The major problem is that, in general, sources are resolved only whilst being lensed. Towards the M31 bulge the stellar surface densities may reach several thousand per arcsec^2 , so after the event one often cannot identify the source to measure its baseline flux. In practice one must monitor pixel flux rather than individual source flux, hence the term *pixel lensing*. Because of the pixel flux contribution of the unlensed sources one typically requires the lensed source to be intrinsically bright or highly magnified, so the majority of microlensing events escape detection. In the high-magnification regime the light-curve suffers from a well-known near-degeneracy in which the excess flux due to microlensing is

$$\Delta F(t) \simeq \frac{A(t_0)F_s}{\sqrt{1 + \left[\frac{t - t_0}{t_e A(t_0)^{-1}} \right]^2}} \quad (A \gtrsim 10), \quad (1)$$

where t denotes observation epoch, t_0 is the epoch at which the magnification, A , attains its maximum, F_s is the baseline source flux and t_e the Einstein radius crossing time. As Woźniak & Paczyński (1997) have pointed out, equation (1) is invariant under transformations $F_s \rightarrow F_s/\alpha$, $A \rightarrow \alpha A$, and $t_e \rightarrow \alpha t_e$ for constants α preserving the high-magnification regime. Under such circumstances one is unable to unambiguously determine t_e , an important observable for conventional microlensing studies. All of this is made worse still by variations in seeing, sky background, detector position and point spread function which make it difficult to isolate the microlensing signal. Changes in seeing pose a severe problem because they induce localized flux variations on timescales comparable to microlensing.

These challenges, though difficult, have been met. Two pilot experiments able to detect true source flux variation on a routine basis have demonstrated the technical viability of pixel lensing (Crotts & Tomaney 1996; Ansari et al. 1997). The experiments employed different techniques, difference imaging and superpixel photometry, to compensate for changes in seeing. However, the limiting factor for both surveys has been the small field of view, yielding relatively modest statistics.

3. POINT-AGAPE

Building upon the pioneering French AGAPE (Andromeda Galaxy Amplified Pixels Experiment) programme, the Anglo-French POINT-AGAPE survey is employing the INT wide-field camera (WFC) to image a large fraction of the M31 disc (POINT is an acronym for Pixel-lensing Observations with INT). The survey began in August 1999 and is undertaking multi-colour observations in two fields, covering 0.6 deg^2 of the disc. The first season of data collection was completed in January 2000.

We have performed detailed simulations to model the sensitivity of the POINT-AGAPE survey, incorporating the effects of seeing and variable sky background, as well as our sampling (Kerins et al. 2000). The simulations include spherical near-isothermal models for both the Galaxy and M31 haloes, as well as a sech-squared disc and exponential bulge for the M31 stellar components. For the haloes we have simulated the expected signal for a wide range of MACHO masses, whilst for the stellar components we have assumed a Solar neighbourhood mass function.

Simulations of the expected spatial distribution of observed events after three seasons for 0.1 , 1 and $10 M_\odot$ MACHOs are provided in Figure 2. The figure assumes the Galaxy and M31 haloes are full of MACHOs. The POINT-AGAPE fields are shown by the dashed-line templates. Whilst the fields cover about one-fifth of the area of the disc their central location means that about half of all detectable pixel events across the disc should occur within them. The high concentration of events within the inner 5 arcmin is due mostly to bulge-bulge lensing, where as the MACHOs are dispersed over the entire disc. The near-far asymmetry in M31 MACHOs gives rise to a overall asymmetry in the spatial distribution. One can see from Figure 2 how the number of MACHOs increases and the near-far asymmetry becomes more prominent at small mass scales

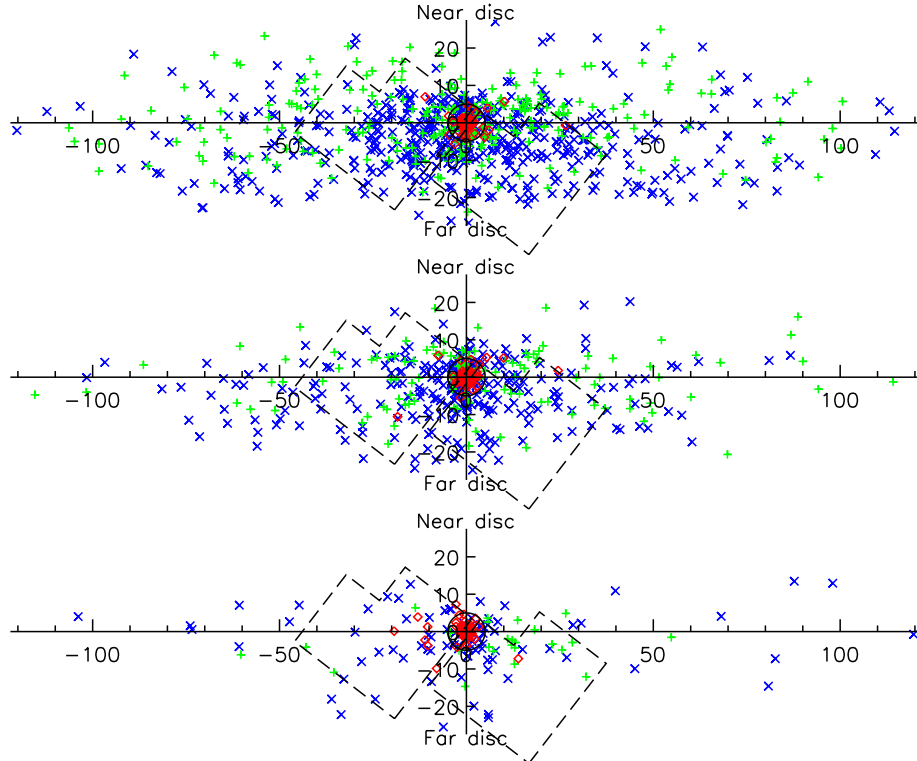
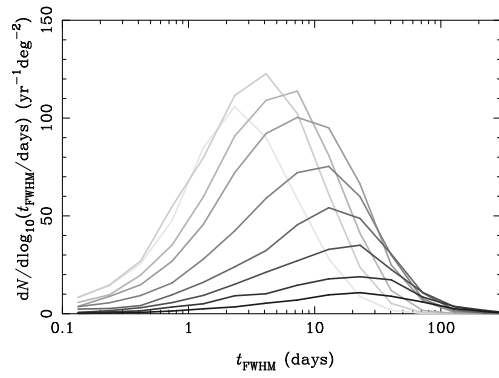


Figure 2. The simulated spatial distribution of pixel-lensing events for the POINT-AGAPE survey after three observing seasons. The axes are in arcmins. Galaxy MACHOs are shown as crosses, M31 MACHOs are depicted by an “x” and stellar events by diamonds. We assume here that MACHOs have a mass of 0.1 (*top*), 1 (*middle*) and $10 M_{\odot}$ (*bottom*) and provide all the dark matter in the Galaxy and M31 haloes. The dashed lines indicate the POINT-AGAPE fields whilst the inner circle denotes the central region dominated by stellar self-lensing.

Figure 3. The combined M31 and Galaxy MACHO t_{FWHM} rate distributions for a range of MACHO masses, normalized to full MACHO haloes and averaged over the M31 disc. From the lightest to the darkest curve the Galaxy and M31 MACHO mass is 0.001, 0.003, 0.01, 0.03, 0.1, 0.3, 1, 3 and $10 M_{\odot}$.



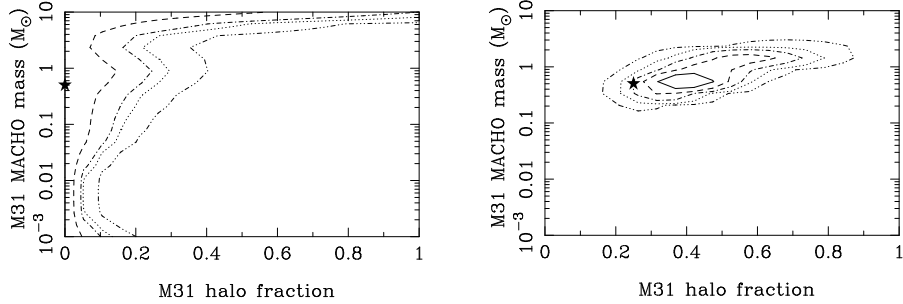
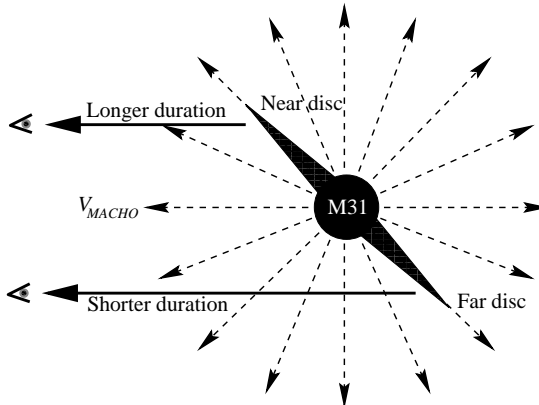


Figure 4. Simulated maximum-likelihood recovery of M31 MACHO parameters. The *left panel* shows the first-season sensitivity of POINT-AGAPE to an absence of near-far asymmetry, and hence an absence of M31 MACHOs (only stellar lensing events and variable stars have been generated in this simulation). In the *right panel* we assume a MACHO mass and contribution as indicated by the star. The contours here illustrate the survey sensitivity after three seasons. For both plots the solid, dashed, dot-dashed, dotted and triple-dot-dashed contours indicate 34%, 68%, 90%, 95% and 99% confidence levels, respectively.

Since the Einstein duration t_e is usually not measurable we have computed the expected event timescale distribution in terms of the full-width at half-maximum flux t_{FWHM} . Figure 3 displays the normalized combined Galaxy and M31 MACHO timescale distribution for a range of mass scales, assuming a maximal MACHO contribution and averaging the rate over the M31 disc. The distributions indicate that the average duration $\langle t_{\text{FWHM}} \rangle$ is sensitive to MACHO mass, though for our sampling it is much less sensitive than the underlying average Einstein duration $\langle t_e \rangle$, with $\langle t_{\text{FWHM}} \rangle \propto \langle t_e \rangle^{1/2}$. The rate peaks for $0.003 - 0.01 M_\odot$ MACHOs, giving ~ 100 events per season for M31 MACHOs and ~ 40 per season for Galaxy MACHOs within the two POINT-AGAPE fields if both haloes are full of MACHOs. If we instead use the most recent Galaxy MACHO mass estimate of $0.5 M_\odot$, with a 20% halo contribution, then we should expect about 15 MACHO detections per season.

We have assessed the extent to which the MACHO mass and halo fraction can be recovered from the observables, specifically the event location and t_{FWHM} . Artificial datasets were constructed from our simulations and a maximum likelihood estimation of MACHO parameters computed using a Bayesian likelihood estimator. As well as M31 MACHOs the datasets include a fixed contribution from stellar lensing and may include Galaxy MACHOs with a different mass and density contribution to the M31 MACHOs. We also make allowances for dataset contamination due to variable stars passing our microlensing selection criteria. Our likelihood estimator is therefore computed over a five-dimensional likelihood space covering M31 MACHO mass and density; Galaxy MACHO mass and density; and a variable star contamination level. In Figure 4 we have summed the likelihood over three of the five dimensions to highlight the sensitivity of

Figure 5. Dual spatial and timescale asymmetry as a probe of velocity anisotropy. If MACHOs have strongly radial orbits then their motion will tend to be parallel to the near-disc sight-line but orthogonal to the far-disc sight-line. Hence near-side events should last longer and have a lower rate, enhancing the spatial asymmetry over that expected for isotropic haloes.



POINT-AGAPE to the M31 MACHO mass and halo fraction. The stars in each panel indicate the input parameters used to generate the artificial dataset whilst the contours indicate the parameter recovery from the dataset. In the left-hand panel our input MACHO fraction is zero, only stellar lensing events and variable stars have been generated. The contours indicate the POINT-AGAPE sensitivity after just one season. Powerful constraints are obtained over a wide range of mass scales due to the lack of any near-far asymmetry. The right-hand panel shows the sensitivity after three seasons for currently favoured MACHO parameters. The constraints on M31 parameters achievable by POINT-AGAPE are comparable to those being obtained for Galaxy MACHOs by the LMC/SMC surveys.

Pixel-lensing surveys towards M31 have the potential not just to probe the halo contribution and mass of MACHOs, but also their distribution function. The near-far asymmetry effect is sensitive to halo flattening, though for highly flattened haloes the asymmetry disappears, making it difficult to distinguish between M31 and Galaxy MACHOs, not to mention variable stars. In Figure 5 we illustrate how near-far asymmetry could also be used to probe the velocity anisotropy of M31 MACHOs. If the MACHOs have strongly radial orbits their trajectories should cut near-side and far-side lines of sight at different angles, giving rise to different characteristic event durations. Specifically, event durations should be longer for the near-side and the rate should be correspondingly reduced (since, for a given optical depth, the rate $\Gamma \propto \langle t_e \rangle^{-1}$) relative to isotropic halo models. In this case we would observe two signatures: an enhanced near-far spatial asymmetry and a near-far timescale asymmetry. This combination of signatures would be difficult to arrange by other means and would therefore represent a strong argument for MACHOs and for an anisotropic MACHO distribution function.

Analysis of the 1999/2000 INT dataset is yet to be finalized, but a preliminary reduction reveals many interesting light-curves, including a variety of variable stars and possible microlensing candidates. Some sample light-curves, spanning about a third of the 1999/2000 baseline, are shown in Figure 6. The light-curves have been processed using superpixel photometry, which is described

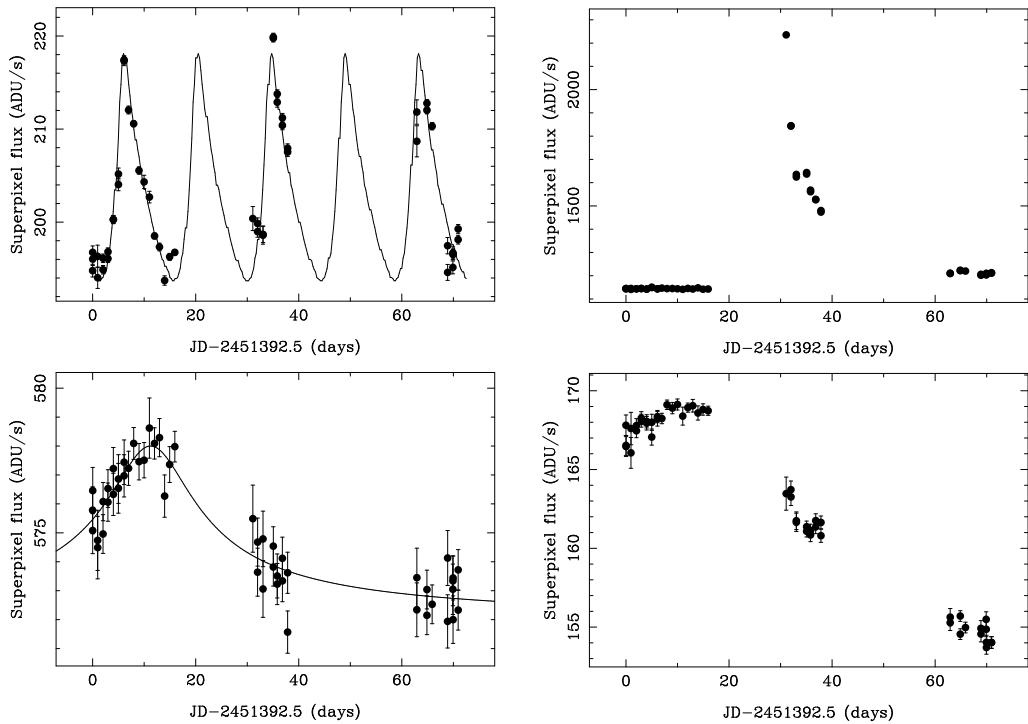


Figure 6. Preliminary r -band light-curves spanning one-third of the 1999/2000 POINT-AGAPE baseline. *Top left*: a possible Cepheid, together with a model fit. *Top right*: a probable nova. *Bottom left*: a light-curve consistent with microlensing, together with a model fit with $t_{\text{FWHM}} = 28$ days. *Bottom right*: another possible microlensing event. A longer baseline is required before either light-curve could be classified as a microlensing candidate.

in detail in Ansari et al. (1997). Briefly, the flux in each pixel is firstly represented by the summed flux over a pixel array, or superpixel, centred on the pixel. The size of the array is set by the size of the pixel relative to the seeing scale, and in the case of the INT WFC a 7×7 superpixel array was chosen. Though this binning dilutes any microlensing signal that may be present it helps to stabilize the effects of seeing variations to a point where a simple linear correction can be applied to the superpixel flux on each image in order to match their seeing characteristics. The method is simple and yet permits differential photometry practically down to the photon noise limit.

The top-left and top-right light-curves in Figure 6 are consistent with a Cepheid and a nova, respectively. They illustrate the high signal-to-noise ratio achievable with INT WFC superpixel photometry. The bottom panels show light-curves consistent with a microlensing interpretation. The light-curve at bottom-left peaks at about $r \simeq 22$ mag and has been fit with a theoretical degenerate microlensing curve with $t_{\text{FWHM}} = 28$ days for illustration. A longer baseline is required before either light-curve could be flagged as a microlensing candidate since long-period variable stars, such as Miras, pose a serious problem

for pixel-lensing selection. To reject such variables one requires at least a three-year baseline. In the short term one can use the presence or absence of near-far asymmetry to statistically measure candidate contamination, since variable stars should have a symmetric spatial distribution.

There are of course limitations to pixel lensing. In common with Galactic microlensing, pixel-lensing constraints are sensitive to the assumed halo distribution function and, as already mentioned, the reduced near-far asymmetry for flattened haloes means that M31 MACHOs in such a configuration will be harder to detect or constrain. The pixel-lensing predictions are additionally sensitive to the shape of the bright end of the M31 stellar luminosity function, which is still to be properly determined. Near-far asymmetry nonetheless remains a very powerful discriminant between MACHOs and stellar self-lensing, an issue which currently hampers the interpretation of the LMC/SMC events. As well as searching for MACHOs, we also hope to be able to constrain the structure and mass function of the M31 bulge, where many self-lensing events are expected to occur. We are optimistic that, within about three seasons, the POINT-AGAPE survey will quantify and constrain both the stellar and MACHO mass function and distribution in M31, furthering our knowledge of the nature of dark matter, and providing a powerful probe of galactic structure.

References

Alcock, C., et al., 1995, *ApJ*, 449, 28
 Alcock, C., et al., 2000, *ApJ* submitted (astro-ph/0001272)
 Ansari, R., et al., 1997, *A&A*, 324, 843
 Baillon, P., Bouquet, A., Giraud-Héraud, Y., Kaplan, J., 1993, *A&A*, 277, 1
 Crotts, A.P.S., 1992, *ApJ*, 399, L43
 Crotts, A.P.S., Tomaney, A., 1996, *ApJ*, 473, L87
 Kerins, E., et al., 2000, *MNRAS*, submitted (astro-ph/0002256)
 Lasserre, T., et al., 2000, *A&A*, submitted (astro-ph/0002253)
 Woźniak, P., Paczynski, B., 1997, *ApJ*, 487, 55